ARTICLE IN PRESS

Nonlinear Analysis: Real World Applications ▮ (▮▮▮▮) ▮▮▮–▮▮▮

Contents lists available at ScienceDirect

Nonlinear Analysis: Real World Applications

journal homepage: www.elsevier.com/locate/nonrwa

Homogenization of long-range auxin transport in plant tissues☆

Andrés Chavarría-Krauser[a,*], Mariya Ptashnyk[a,b]

[a] Institut für Angewandte Mathematik, INF 294, Universität Heidelberg, D-69120 Heidelberg, Germany
[b] Mathematical Institute, University of Oxford, 24-29 St Giles, OX1 3LB, UK

ARTICLE INFO

Article history:
Received 24 January 2008
Accepted 5 December 2008

Keywords:
Homogenization
Diffusion-reaction equation
Plant tissues
Ion transport
Auxin

ABSTRACT

A model for the cell-to-cell transport of the plant hormone auxin is presented. Auxin is a weak acid which dissociates into ions in the aqueous cell compartments. A microscopic model is defined by diffusion-reaction equations and a Poisson equation for a given charge distribution. The microscopic properties of the plant cell were taken into account through oscillating coefficients in the model. Via formal asymptotic expansion a macroscopic model was obtained. The effective diffusion coefficients and transport velocities are expressed by the solution of unit cell problems. Published experimental values of diffusivity and permeability were used to determine numerically the effective transport coefficients and the calculated transport velocity was shown to be of the same order as measured values.

1. Introduction

Auxins belong to the most important plant hormones and play a central role in growth and development regulation (for a review see e.g. [5]). There are several synthetic and natural auxins, the most prominent probably being indole-3-acetic acid (IAA, denominated also simply as auxin in the sequel). IAA is mostly produced in the plant shoot and is transported polarly from cell to cell through the shoot and stem towards the primary root [6]. This transport occurs over several centimeters and extends over thousands of cells.

Quantitative description of auxin transport has been based up-to-date on the *chemiosmotic model of polar auxin diffusion*, proposed in the mid 1970s, [7–9]. The chemiosmotic model uses the fact that IAA is a weak acid and in its ionic form it cannot freely pass through the cell membrane. IAA can enter the cell either as protonated molecules (through passive diffusion) or as ions (through transport proteins). Once in the cell, IAA will dissociate almost completely in the slightly alkaline cytoplasm and can hence exit the cell only through transport proteins. Polarity arises through an asymmetric distribution of the transport proteins. The chemiosmotic model predicted the existence of efflux and influx transporter proteins, [10], which have been observed experimentally in the last decade, [11,12], and describes sufficiently well the transport of radioactively labeled auxin through plant tissues, [13,8]. The mathematical approach used in the chemiosmotic model is to describe either the cells or even cell compartments (cell wall, cell membrane, cytoplasm, vacuole; cmp. Fig. 1) as discrete objects. This approach has led to some open questions, the most remarkable is probably whether auxin transport has a velocity, [7]. Until now the movement of the center of mass of simulated auxin pulses has been used to assign a velocity of transport. This approach is imprecise and does not show the existence of a true transport velocity.

The article presented here focuses on the extension of the chemiosmotic model by usage of a multiscale approach to finally define a macroscopic average velocity of long-range auxin transport. Using conservation of protonated auxin and auxin ions, a microscopic model describing the diffusion, reaction and electric flux is posed. We assume that the plant tissue

☆ Supported by "Center for Modeling and Simulation in the Biosciences" (BIOMS).
* Corresponding author.
E-mail addresses: andres.chavarria@bioquant.uni-heidelberg.de (A. Chavarría-Krauser), mariya.ptashnyk@iwr.uni-heidelberg.de (M. Ptashnyk).

1468-1218/$ – see front matter © 2009 Elsevier Ltd. All rights reserved.
doi:10.1016/j.nonrwa.2008.12.003

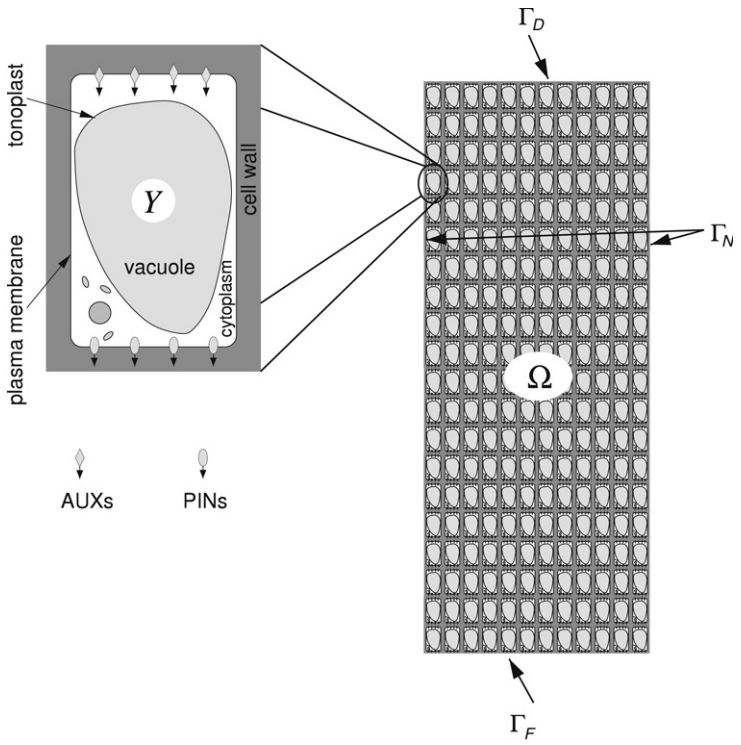

Fig. 1. Unity cell Y, which corresponds to a biological cell, and tissue represented by the microscopic domain Ω with corresponding boundaries (Γ_N, Γ_D and Γ_F). Influx (AUXs) and efflux (PINs) transport proteins are distributed asymmetrically on the plasma membrane.

is composed periodically of identical plant cells. The microscopic properties of the plant cells are reflected by oscillating coefficients in the model. A macroscopic model is obtained by means of a formal asymptotic expansion. Related results on asymptotic analysis of diffusion-convection equations can be found in [14–16]. The solutions of unit cell problems determine the macroscopic diffusion coefficients and transport velocity, which allow one to do numerical simulations which relate the distribution and permeability of transport proteins with the effective velocity.

2. Microscopic description

The situation modeled here is described in Fig. 1. The plant tissue is assumed to be composed periodically of identical plant cells. The internal structure of these plant cells is assumed to consist of cell wall, a plasma membrane, cytoplasm, tonoplast and a vacuole. On the membrane we assume that two kinds of transport protein are present: influx (AUXs/LAXs) and efflux (PINs) proteins.

IAA is a weak acid and dissociates in aqueous solutions. The dissociation rate is independent of pH. However the recombination rate depends on the amount of protons in the solution and hence on the pH value. We assume following reaction

$$\mathrm{IAAH} \underset{r_r}{\overset{r_d}{\rightleftharpoons}} \mathrm{IAA}^- + \mathrm{H}^+,$$

where $r_d = \text{const}$ and $r_r = r_r(pH)$ are the dissociation and recombination rates, respectively. The pH value depends on the cell compartment and therefore the equilibrium shifts towards dissociated auxin (in cytoplasm) or protonated auxin (in cell wall and vacuole). The concentration of the ion IAA^- will be denoted by u, while v is the concentration of the protonated auxin IAAH. We assume that there is no bulk flow and that both IAAH and IAA^- diffuse. The diffusion coefficients will be denoted by D_u and D_v, respectively. Due to the negative charge of the ions, the electric potential differences across the plasma membrane and tonoplast produce an additional flux of IAA^-. The mobility of the ions is given by the permeability P, which determines together with the electric field ϕ and u, the electric flux $P\,u\,\phi$. The concentrations u and v are in the order of 1 nM, while other ions (in particular K^+, Na^+ and Cl^-) appear in concentrations of 1 mM. Therefore we can assume that the electric field inside a cell is independent of u and is generated by the equilibrium membrane potential produced by the other ions (ca. −120 mV between cell wall and cytoplasm and 50 mV between cytoplasm and vacuole). Moreover the equilibrium membrane potential is assumed to be stationary.

Thus the diffusion and transport of IAA^- and IAA is described by the following equations

$$\partial_t u + \operatorname{div}(P\,\phi\,u) - \operatorname{div}(D_u\,\nabla u) = r_d\,v - r_r\,u,$$

Please cite this article in press as: A. Chavarría-Krauser, M. Ptashnyk, Homogenization of long-range auxin transport in plant tissues, Nonlinear Analysis: Real World Applications (2009), doi:10.1016/j.nonrwa.2008.12.003

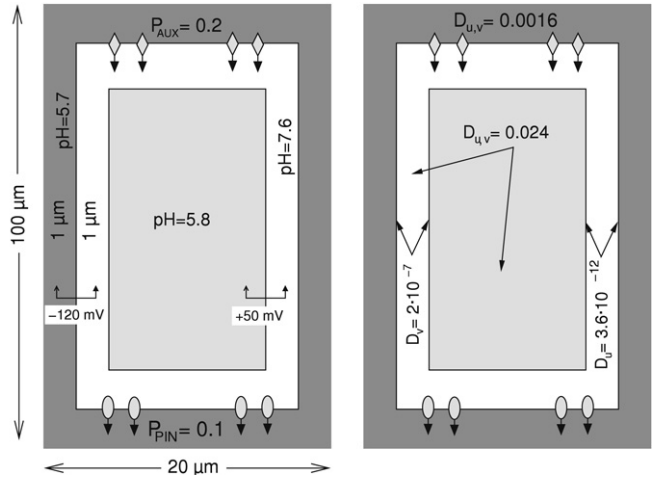

Fig. 2. Simplified geometry and parameters used in simulation. Units: $[P_{PIN}] = [P_{AUX}] = \text{cm h}^{-1}$, $[D_u] = [D_v] = \text{cm}^2\ \text{h}^{-1}$.

$$\partial_t v - \operatorname{div}(D_v \nabla v) = -r_d\, v + r_r\, u, \qquad \operatorname{div}\phi = \rho, \tag{1}$$

where $\rho = \rho(x)$ is only a function of the space variable.

In the single cell we have five different domains (Figs. 1 and 2). The order of the coefficients can vary substantially between these domains. In the cell wall diffusion coefficients $D_{u,v}$ are ca. $D_w/15$, where D_w is the diffusion coefficient of auxin in water, in the plasma membrane and tonoplast $D_{u,v}$ is ca. $D_w \times 10^{-10}$ and in the vacuole and in the cytoplasm $D_{u,v} \approx D_w$. The electric field is about $10^5\ \text{V cm}^{-1}$ in the plasma membrane, $5 \times 10^4\ \text{V cm}^{-1}$ in the tonoplast and almost zero elsewhere. The permeability P is of the order of $3 \times 10^{-6}\ \text{cm}^2\ \text{V}^{-1}\ \text{h}^{-1}$. The thickness of the cell wall and cytoplasm is 10^{-4} cm, the thickness of the membranes is 10^{-6} cm. Thus $D\nabla u_0$ is proportional to $16\, u_0$ in the cell wall, to $240\, u_0$ in cytoplasm and 10^{-9} in the membranes. For the transport term we obtain $P\phi u_0 \approx 0.3\, u_0$ to $30\, u_0$ in the plasma membrane. The dissociation and recombination of auxin is very fast and for the reaction rates we have $r_d \approx 5 \times 10^9\ \text{h}^{-1}$ and $r_r \approx 5 \times 10^6$ to $5 \times 10^8\ \text{h}^{-1}$.

Let $\Omega = (0, 1) \times (0, 10) \times (0, 1)$ represent the plant tissue. The ratio between the size of the cells and the size of the whole domain Ω is denoted as $\varepsilon > 0$ (here $\varepsilon \approx \frac{100\ \mu\text{m}}{10\ \text{cm}} = 10^{-3}$). Choosing the characteristic reaction time as the time scale in the model, the flux terms have to be scaled by ε.

We consider the so-called "standard cell", $Y = [0, 2] \times [0, 10] \times [0, 2]$ (cmp. Fig. 2 and $\varepsilon = 10^{-3}$), periodically repeated over $\mathbb{R}^3$ and define, for $k \in \mathbb{Z}^3$ and vectors q_i (with $q_1 = 2\,e_1$, $q_2 = 10\,e_2$ and $q_3 = 2\,e_3$), $Y^k = Y + \sum_{i=1}^3 k_i q_i$, and $\Omega = \cup\{\varepsilon Y^k | \varepsilon Y^k \subset \Omega, k \in \mathbb{Z}^3\}$.

The coefficients in the equations are defined by the Y-periodic functions $P^\varepsilon(x) = P(\frac{x}{\varepsilon})$, $\rho^\varepsilon(x) = \rho(\frac{x}{\varepsilon})$, $D_u^\varepsilon(x) = D_u(\frac{x}{\varepsilon})$, $D_u^\varepsilon(x) = D_u(\frac{x}{\varepsilon})$, $R_d^\varepsilon(x) = R_d(\frac{x}{\varepsilon}) = \varepsilon^{-1} r_d(\frac{x}{\varepsilon})$, $R_r^\varepsilon(x) = R_r(\frac{x}{\varepsilon}) = \varepsilon^{-1} r_r(\frac{x}{\varepsilon})$.

We assume that the potential $\rho \in L^\infty(Y)$, ρ is periodic in Y, and $\int_Y \rho(y)\mathrm{d}y = 0$. Then we consider a problem

$$\Delta\varphi = \rho \quad \text{in } Y, \qquad \varphi \quad \text{is periodic in } Y. \tag{2}$$

The existence and regularity theory for elliptic equations implies the existence of a solution $\varphi(y)$, periodic in Y and Lipschitz continuous, [17]. We extend φ periodically from Y into $\mathbb{R}^3$ and define the microscopic electric field by

$$\phi^\varepsilon = \varepsilon \nabla_x \varphi\left(\frac{x}{\varepsilon}\right). \tag{3}$$

Although φ is determined up to an additive constant, the electric field ϕ^ε is uniquely defined.

Then, due to the Eq. (2) and the appropriate scaling of the coefficients in (1), the microscopic equations for IAA^- and $IAAH$ are

$$\begin{aligned}
&\partial_t u^\varepsilon + \varepsilon \operatorname{div}(P^\varepsilon \phi^\varepsilon u^\varepsilon) - \varepsilon \operatorname{div}\left(D_u^\varepsilon \nabla u^\varepsilon\right) = R_d^\varepsilon v^\varepsilon - R_r^\varepsilon u^\varepsilon \quad \text{in } (0, T) \times \Omega,\\
&\partial_t v^\varepsilon - \varepsilon \operatorname{div}\left(D_v^\varepsilon \nabla v^\varepsilon\right) = -R_d^\varepsilon v^\varepsilon + R_r^\varepsilon u^\varepsilon \quad \text{in } (0, T) \times \Omega,\\
&\varepsilon \operatorname{div}\phi^\varepsilon = \rho^\varepsilon \quad \text{in } \Omega,\\
&u^\varepsilon = u_D \quad \text{on } \Gamma_D,\\
&v^\varepsilon = v_D \quad \text{on } \Gamma_D,\\
&(P^\varepsilon \phi^\varepsilon u^\varepsilon - D^\varepsilon \nabla u^\varepsilon) \cdot \nu = 0 \quad \text{on } \Gamma_N,\\
&\nabla v^\varepsilon \cdot \nu = 0 \quad \text{on } \Gamma_N,
\end{aligned} \tag{4}$$

Please cite this article in press as: A. Chavarría-Krauser, M. Ptashnyk, Homogenization of long-range auxin transport in plant tissues, Nonlinear Analysis: Real World Applications (2009), doi:10.1016/j.nonrwa.2008.12.003

$$
\begin{aligned}
&(P^\varepsilon \phi^\varepsilon u^\varepsilon - D^\varepsilon \nabla u^\varepsilon)\cdot \nu = u^\varepsilon c\cdot \nu \quad \text{on } \Gamma_F,\\
&\nabla v^\varepsilon \cdot \nu = v^\varepsilon c\cdot \nu \quad \text{on } \Gamma_F,\\
&u^\varepsilon,\quad v^\varepsilon \quad \text{periodic in } x_3,\\
&u^\varepsilon = u_{\text{int}},\qquad v^\varepsilon = v_{\text{int}} \quad \text{in } \Omega^\varepsilon.
\end{aligned}
$$

Definition 2.1. The weak solution of the problem (4) is given by the functions u^ε, $v^\varepsilon \in H^1(0,T;L^2(\Omega))$, $u^\varepsilon - u_D$, $v^\varepsilon - v_D \in L^2(0,T;W(\Omega))$ such that

$$
\begin{aligned}
&\int_0^T\int_\Omega \partial_t u^\varepsilon \psi \,\mathrm{d}x\mathrm{d}t + \varepsilon\int_0^T\int_\Omega (-P^\varepsilon\phi^\varepsilon u^\varepsilon \nabla\psi + D_u^\varepsilon \nabla u^\varepsilon\nabla\psi)\mathrm{d}x\mathrm{d}t\\
&\quad + \int_0^T\int_{\Gamma_F} u^\varepsilon c\cdot\nu \,\mathrm{d}\gamma\mathrm{d}t = \int_0^T\int_\Omega (R_d^\varepsilon v^\varepsilon - R_r^\varepsilon u^\varepsilon)\psi\,\mathrm{d}x\mathrm{d}t,\\
&\int_0^T\int_\Omega \partial_t v^\varepsilon \psi\,\mathrm{d}x\mathrm{d}t + \varepsilon\int_0^T\int_\Omega D_v^\varepsilon\nabla v^\varepsilon\nabla\psi\,\mathrm{d}x\mathrm{d}t + \int_0^T\int_{\Gamma_F} v^\varepsilon c\cdot\nu\mathrm{d}\gamma\mathrm{d}t\\
&\quad = \int_0^T\int_\Omega (-R_d^\varepsilon v^\varepsilon + R_r^\varepsilon u^\varepsilon)\,\psi\,\mathrm{d}x\mathrm{d}t
\end{aligned}
\tag{5}
$$

for all $\psi \in L^2(0,T;W(\Omega))$, for $\phi^\varepsilon \in L^\infty(\Omega)$ given by (3), and u^ε, v^ε satisfy the initial conditions, i.e. $u^\varepsilon \to u_{\text{int}}$, $v^\varepsilon \to v_{\text{int}}$ in $L^2(\Omega)$ as $t \to 0$.

Here

$$W(\Omega) = \{v \in H^1(\Omega),\ v = 0 \text{ on } \Gamma_D\}.$$

To ensure the existence of the solution of system (4) the following assumptions on the coefficients and initial data are needed

Assumption 2.2.
- Diffusion coefficients $D_u, D_v \in L^\infty(Y)$ are uniformly elliptic, i.e. $D_u\xi\xi \geq d_0|\xi|^2$, $D_v\xi\xi \geq d_0|\xi|^2$ for $\xi \in \mathbb{R}^3$.
- Permeability $P \in L^\infty(Y)$, and outflow velocity $c \in H^1(0,T;L^\infty(\Gamma_F))$.
- Reaction rates R_u, $R_v \in L^\infty(Y)$.
- Boundary conditions u_D, $v_D \in H^1(0,T;H^1(\Omega))$, and initial condition u_{int}, $v_{\text{int}} \in H^1(\Omega)$.

Theorem 2.3. *Under the Assumption 2.2 for each fixed ε there exists a unique weak solution of the problem (4).*

Proof. For given $\phi^\varepsilon \in L^\infty(\Omega)$ the existence of a unique weak solution of Eq. (4) with bounded vector field and Robin boundary conditions follows from Theorem 5.1 in [18] or Theorem 6.39 in [19] combined with a priori estimates for $\partial_t u^\varepsilon$ and $\partial_t v^\varepsilon$ similar to the Theorem 6.1, [18], for Dirichlet boundary conditions. □

3. Macroscopic model

Macroscopic equations are gained using the Ansatz of asymptotic expansion $u^\varepsilon(x) = u_0(x,y) + \varepsilon u_1(x,y) + \mathcal{O}(\varepsilon^2)$, $v^\varepsilon(x) = v_0(x,y) + \varepsilon v_1(x,y) + \mathcal{O}(\varepsilon^2)$ and $\phi^\varepsilon(x) = \phi_0(y) + \varepsilon\phi_1(y) + \mathcal{O}(\varepsilon^2)$, where the functions u_i, v_i, ϕ_i are periodic with respect to the microscopic fast variable $y = x/\varepsilon$ and $\nabla = \nabla_x + \frac{1}{\varepsilon}\nabla_y$. We obtain thus for the order $\mathcal{O}(\varepsilon^{-1})$ the equations

$$
\begin{aligned}
&\nabla_y\cdot\left(D_u\,\nabla_y u_0\right) = 0,\\
&\nabla_y\cdot\left(D_v\,\nabla_y v_0\right) = 0
\end{aligned}
$$

with periodic boundary conditions. This implies that the functions u_0 and v_0 do not depend on the microscopic variable y and are functions of the macroscopic variable x. The next order in the expansion gives

$$
\begin{aligned}
&\partial_t u_0 - \nabla_y\cdot\left(D_u\,\nabla_y u_1 + D_u\nabla_x u_0\right) + \nabla_y\cdot(P\,\phi_0\,u_0) - \nabla_x\cdot\left(D_u\,\nabla_y u_0\right) = R_d\,v_0 - R_r\,u_0,\\
&\partial_t v_0 - \nabla_y\cdot\left(D_v\,\nabla_y v_1 + D_v\,\nabla_x v_0\right) - \nabla_x\cdot\left(D_v\,\nabla_y v_0\right) = -R_d\,v_0 + R_r\,u_0,\\
&\nabla_y\cdot\phi_0 = \rho.
\end{aligned}
\tag{6}
$$

By the Fredholm alternative, the equations in (6), as elliptic equations in y with periodic boundary conditions, have a solution if and only if

$$
\begin{aligned}
&\partial_t u_0 = \langle R_d\rangle\,v_0 - \langle R_r\rangle\,u_0,\\
&\partial_t v_0 = -\langle R_d\rangle\,v_0 + \langle R_r\rangle\,u_0,
\end{aligned}
\tag{7}
$$

where $\langle R_d\rangle = \frac{1}{|Y|}\int_Y R_d\,\mathrm{d}y$ and $\langle R_r\rangle = \frac{1}{|Y|}\int_Y R_r\mathrm{d}y$ and u_0 and v_0 fulfill initial conditions

$$u_0 = u_{\text{int}},\qquad v_0 = v_{\text{int}} \quad \text{for } t = 0.$$

Please cite this article in press as: A. Chavarría-Krauser, M. Ptashnyk, Homogenization of long-range auxin transport in plant tissues, Nonlinear Analysis: Real World Applications (2009), doi:10.1016/j.nonrwa.2008.12.003

The Eq. (7) represents the dissociation and recombination of auxin. Since the reaction rates are much faster than transport and diffusion, it was expected that the zero order approximations u_0 and v_0 are solutions of ordinary differential equations. Due to regularity of initial conditions we obtain that $u_0, v_0 \in C^1(0, T; H^1(\Omega))$.

In order to see the influence of transport and diffusion on the solution and also to define the auxin transport velocity, we consider the terms of $\mathcal{O}(\varepsilon)$ in the asymptotic expansion and find u_1 and v_1. Using the expression for $\partial_t u_0$ and $\partial_t v_0$ from (7) in the Eq. (6) we obtain

$$\begin{aligned} -\nabla_y \cdot \left(D_u \nabla_y u_1 + D_u \nabla_x u_0\right) + \nabla_y \cdot (P \phi_0 u_0) &= (R_d - \langle R_d \rangle)\ v_0 - (R_r - \langle R_r \rangle)\ u_0, \\ -\nabla_y \cdot \left(D_v \nabla_y v_1 + D_v \nabla_x v_0\right) &= -(R_d - \langle R_d \rangle)\ v_0 + (R_r - \langle R_r \rangle)\ u_0. \end{aligned} \tag{8}$$

The system (8) is composed of linear elliptic equations in respect to y, where zero order terms are proportional to $\nabla_x u_0$, $\nabla_x v_0$, u_0, and v_0. This structure suggests the Ansatz

$$\begin{aligned} u_1(t,x,y) &= w_u(y) \cdot \nabla_x u_0(t,x) + Z_{uu}(y)\, u_0(t,x) + Z_{uv}(y)\, v_0(t,x) + \bar{u}_1(t,x), \\ v_1(t,x,y) &= w_v(y) \cdot \nabla_x v_0(t,x) + Z_{vu}(y)\, u_0(t,x) + Z_{vv}(y)\, v_0(t,x) + \bar{v}_1(t,x), \end{aligned}$$

and from (8) we obtain the unit cell problems

$$\begin{aligned} &\nabla_y \cdot \left(D_\alpha \nabla_y w_{\alpha j}\right) = -\nabla_y \cdot \left(D_\alpha\, e_j\right) \quad \text{for } \alpha = \{u, v\} \\ &\nabla_y \cdot \left(D_u \nabla_y Z_{uu}\right) = (R_r - \langle R_r \rangle) + \nabla_y \cdot (P \phi_0) \\ &\nabla_y \cdot \left(D_u \nabla_y Z_{uv}\right) = -(R_d - \langle R_d \rangle) \\ &\nabla_y \cdot \left(D_v \nabla_y Z_{vu}\right) = -(R_r - \langle R_r \rangle) \\ &\nabla_y \cdot \left(D_v \nabla_y Z_{vv}\right) = (R_d - \langle R_d \rangle) \\ &w_{\alpha j}, Z_{uu}, Z_{uv}, Z_{vu}, Z_{vv} \quad \text{periodic and fulfilling} \\ &\int_Y w_{\alpha j} \mathrm{d}y = 0, \qquad \int_Y Z_{uu} \mathrm{d}y = 0, \qquad \int_Y Z_{uv} \mathrm{d}y = 0, \qquad \int_Y Z_{vu} \mathrm{d}y = 0, \qquad \int_Y Z_{vv} \mathrm{d}y = 0. \end{aligned} \tag{9}$$

For terms of order ε we obtain following equations

$$\begin{aligned} &\partial_t u_1 - \nabla_y \cdot \left(D_u \nabla_y u_2 + D_u \nabla_x u_1\right) + \nabla_y \cdot (P \phi_0 u_1 + P \phi_1 u_0) \\ &\quad - \nabla_x \cdot \left(D_u \nabla_y u_1 + D_u \nabla_x u_0\right) + \nabla_x \cdot (P \phi_0 u_0) = R_d\, v_1 - R_r\, u_1, \\ &\partial_t v_1 - \nabla_y \cdot \left(D_v \nabla_y v_2 + D_v \nabla_x v_1\right) - \nabla_x \cdot \left(D_v \nabla_y v_1 + D_v \nabla_x v_0\right) = -R_d\, v_1 + R_r\, u_1, \\ &\nabla_y \cdot \phi_1 = 0. \end{aligned} \tag{10}$$

Using the Ansatz for $u_1(t,x,y)$ and $v_1(t,x,y)$, the zero mean values assumption on w_α and $Z_{\alpha\beta}$ and the solvability condition for (10) we obtain the equations for the nonoscillating terms $\bar{u}_1(t,x)$ and $\bar{v}_1(t,x)$

$$\begin{aligned} \partial_t \bar{u}_1 - \mathrm{div}\,(\mathcal{A}_u \nabla u_0) + \mathrm{div}\,(\mathcal{V}_{uu}\, u_0) + \mathrm{div}\,(\mathcal{V}_{uv}\, v_0) &= \langle R_d \rangle\, \bar{v}_1 - \langle R_r \rangle\, \bar{u}_1 + \mathcal{R}_r\, u_0 - \mathcal{R}_d\, v_0, \\ \partial_t \bar{v}_1 - \mathrm{div}\,(\mathcal{A}_v \nabla v_0) + \mathrm{div}\,(\mathcal{V}_{vu}\, u_0) + \mathrm{div}\,(\mathcal{V}_{vv}\, v_0) &= -\langle R_d \rangle\, \bar{v}_1 + \langle R_r \rangle\, \bar{u}_1 + \mathcal{R}_d\, v_0 - \mathcal{R}_r\, u_0, \end{aligned} \tag{11}$$

where the effective coefficients are defined

$$\begin{aligned} \mathcal{A}_\alpha &= \frac{1}{|Y|} \int_Y D_\alpha \left(\nabla_y w_\alpha + \mathbf{I}\right) \mathrm{d}y \\ \mathcal{V}_{uu} &= \frac{1}{|Y|} \int_Y \left(-D_u \nabla_y Z_{uu} + R_r\, w_u + P^\varepsilon \phi_0\right) \mathrm{d}y \\ \mathcal{V}_{uv} &= -\frac{1}{|Y|} \int_Y \left(D_u \nabla_y Z_{uv} + R_d\, w_v\right) \mathrm{d}y \\ \mathcal{V}_{vu} &= -\frac{1}{|Y|} \int_Y \left(D_v \nabla_y Z_{vu} + R_r\, w_u\right) \mathrm{d}y \\ \mathcal{V}_{vv} &= \frac{1}{|Y|} \int_Y \left(-D_v \nabla_y Z_{vv} + R_d\, w_v\right) \mathrm{d}y \\ \mathcal{R}_d &= \frac{1}{|Y|} \int_Y (R_r\, Z_{uv} - R_d\, Z_{vv})\, \mathrm{d}y \\ \mathcal{R}_r &= \frac{1}{|Y|} \int_Y (R_d\, Z_{vu} - R_r\, Z_{uu})\, \mathrm{d}y. \end{aligned} \tag{12}$$

Please cite this article in press as: A. Chavarría-Krauser, M. Ptashnyk, Homogenization of long-range auxin transport in plant tissues, Nonlinear Analysis: Real World Applications (2009), doi:10.1016/j.nonrwa.2008.12.003

Table 1
Simulation parameters. Diffusion coefficient of auxin in water is $D_w = 0.024\,\mathrm{cm^2 h^{-1}}$. Units: $[D_u^\varepsilon] = [D_v^\varepsilon] = \mathrm{cm^2\ h^{-1}}$, $[R_d^\varepsilon] = [R_r^\varepsilon] = \mathrm{h^{-1}}$, $[|\phi^\varepsilon|] = V\ \mathrm{cm^{-1}}$, $[P^\varepsilon] = \mathrm{cm\ h^{-1}}$.

Parameter	Cell wall	Plasma membrane		Cytoplasm	Tonoplast	Vacuole
pH	5.8	–		7.6	5.7	
D_u^ε	$\frac{D_w}{15}$	3.6×10^{-12}		D_w	3.6×10^{-12}	D_w
D_v^ε	$\frac{D_w}{15}$	2×10^{-7}		D_w	2×10^{-7}	D_w
R_d^ε	5×10^9	5×10^9		5×10^9	5×10^9	5×10^9
$\lvert\phi^\varepsilon\rvert$	0	120×10^3		0	50×10^3	0
Permeability		P_{PIN}	P_{AUX}		P_{Ton}	
		0.1	0.2		0.2	

References: [1–4].

Then for the nonoscillating part of the first two terms in u^ε, v^ε, i.e. $u_1^\varepsilon(t,x) = u_0(t,x) + \varepsilon\bar{u}_1(t,x)$ and $v_1^\varepsilon(t,x) = v_0(t,x) + \varepsilon\bar{v}_1(t,x)$ we obtain the equations

$$\begin{aligned}
&\partial_t u_1^\varepsilon - \varepsilon\,\mathrm{div}\,(\mathcal{A}_u\nabla u_0) + \varepsilon\,\mathrm{div}\,(\mathcal{V}_{uu}\,u_0) + \varepsilon\,\mathrm{div}\,(\mathcal{V}_{uv}\,v_0) = \langle R_d\rangle\,v_1^\varepsilon - \langle R_r\rangle\,u_1^\varepsilon + \varepsilon(\mathcal{R}_r\,u_0 - \mathcal{R}_d\,v_0),\\
&\partial_t v_1^\varepsilon - \varepsilon\,\mathrm{div}\,(\mathcal{A}_v\nabla v_0) + \varepsilon(\mathrm{div}\,(\mathcal{V}_{vu}\,u_0) + \mathrm{div}\,(\mathcal{V}_{vv}\,v_0)) = -\langle R_d\rangle\,v_1^\varepsilon + \langle R_r\rangle\,u_1^\varepsilon + \varepsilon(\mathcal{R}_d\,v_0 - \mathcal{R}_r\,u_0)
\end{aligned} \tag{13}$$

with boundary conditions

$$\begin{aligned}
&-\varepsilon(\mathcal{A}_u\nabla u_0 - \mathcal{V}_{uu}u_0 - \mathcal{V}_{uv}v_0)\cdot\nu = \varepsilon c\cdot\nu u_0 \quad \text{on } \Gamma_F,\\
&-\varepsilon(\mathcal{A}_v\nabla v_0 - \mathcal{V}_{vu}u_0 - \mathcal{V}_{vv}v_0)\cdot\nu = \varepsilon c\cdot\nu v_0 \quad \text{on } \Gamma_F,\\
&-\varepsilon(\mathcal{A}_u\nabla u_0 - \mathcal{V}_{uu}u_0 - \mathcal{V}_{uv}v_0)\cdot\nu = 0 \quad \text{on } \Gamma_N,\\
&-\varepsilon(\mathcal{A}_v\nabla v_0 - \mathcal{V}_{vu}u_0 - \mathcal{V}_{vv}v_0)\cdot\nu = 0 \quad \text{on } \Gamma_N,\\
&u_0,\ v_0 \quad \text{periodic in } x_3,
\end{aligned}$$

and initial conditions

$$u_1^\varepsilon(0,x) = u_{\mathrm{int}}(x), \qquad v_1^\varepsilon(0,x) = v_{\mathrm{int}}(x).$$

Since the zero-order terms solve ordinary differential equations, the approximative solution u_1^ε, v_1^ε does not fulfill the Dirichlet boundary conditions. The natural idea to correct the boundary effect would be to construct boundary layer functions. But the corresponding boundary layer functions will decay exponentially to a nonzero constant and create additional error. This indicates that inflow boundary conditions should be defined in a different way than Dirichlet boundary conditions and provide new prospects for a further modeling. Additionally we have only boundedness of coefficients in the model. For proving the error estimates between original and homogenized solutions more regularity of coefficients would be needed. Since the main aim of the present work is to define macroscopic equations and to find an expression for the effective transport velocities, we are not considering the error estimates here.

4. Simulation

4.1. Geometry

For simplicity the problem was simulated in two dimensions (Fig. 2). A quadratic plant cell of length 100 μm and width 20 μm was used, because it represents the typical size of auxin transporting cells in maize coleoptiles, [20]. The cell wall and the cytoplasm were assumed to be 1 μm thick and the membranes, i.e. plasma membrane and tonoplast, were chosen to be 10 nm thick.

4.2. Parameters

A slightly acidic pH is found in the cell wall and vacuole, while the pH in the cytoplasm is slightly alkaline (compare Fig. 2 and Table 1). Therefore the recombination rate R_r^ε oscillates in space. The reaction rates R_d^ε and R_r^ε are not independent, as these can be expressed by the dissociation rate as follows

$$R_r^\varepsilon = R_d\,10^{pKa - pH^\varepsilon}, \tag{14}$$

where $pKa = 4.75$ is the acid dissociation constant of auxin. No published value for the dissociation rate of auxin is known to the authors. However, the dissociation rate of weak acids seems to depend linearly on the pKa value of the acid, [3]. Therefore the dissociation rate R_d was assumed here to be constant and was chosen as $5 \times 10^9\ \mathrm{h^{-1}}$, [3].

The diffusion coefficient of auxin in water is $D_w = 0.024\,\mathrm{cm^2 h^{-1}}$, [2]. As a rough approximation, we assume that both the ion and protonated auxin have similar diffusion coefficients in aqueous solutions. The cell wall is a very complex anisotropic layered polymer. Diffusion inside the cell wall is therefore a complex process which would deserve a treatment by itself and

Please cite this article in press as: A. Chavarría-Krauser, M. Ptashnyk, Homogenization of long-range auxin transport in plant tissues, Nonlinear Analysis: Real World Applications (2009), doi:10.1016/j.nonrwa.2008.12.003

is therefore outside the scope of this paper. Until now, diffusion coefficients have been determined experimentally without taking the microstructure of the cell wall into account, [2]. We therefore use here for both the cell wall and cytoplasm scalar diffusion coefficients (Fig. 2 and Table 1).

We use here the constant field approximation for the electric field, [21], which assumes a constant field inside the membrane. Moreover, as a rough approximation, we assume that the field is zero outside the membrane. A membrane potential of −120 mV between the cell wall and the cytoplasm, and of +50 mV between the cytoplasm and the vacuole were used. Compare Fig. 2 and Table 1. The mobility of the ions is given by the permeability P^ε

$$P^\varepsilon = -\frac{z\,F}{R\,T}\left(D_u^\varepsilon + h_m\,(P_{PIN}^\varepsilon - P_{AUX}^\varepsilon)\right), \tag{15}$$

where $z = -1$ is the valence of the ion, $F = 96485.3383$ C mol^{-1} is the Faraday constant, $R = 8.314472$ J K^{-1} mol^{-1} is the ideal gas constant, $T = 300\ K$ is the temperature, $h_m = 10^{-6}$ cm is the membrane thickness, P_{PIN}^ε and P_{AUX}^ε are the permeabilities of the efflux and influx transport proteins, respectively (Table 1).

4.3. Results

The cell problems (9) were solved using a discrete difference method, which is equivalent to a finite volume method for a regular grid. The numerical treatment of the membrane and tonoplast deserve more attention, because of their small thickness. If sufficiently small finite volumes are used, then the membrane can be resolved. However, the membrane is very thin compared to the characteristic size of Y, which would result in huge amounts of finite volumes. Another approach is to use non-uniform discretizations, which need substantially more programming effort. Due to the strong difference between the diffusion coefficients in the membrane and outside, it is possible to use a standard finite volume method on a uniform grid. The reason for this will be outlined in the following paragraph.

In the spirit of the finite volume method, for each finite volume, a volume integral of the divergence $\nabla_y \cdot (D_\alpha\,\nabla_y\,\cdot)$ in Eq. (9) is converted into a integral of the flux $n \cdot D_\alpha\,\nabla_y\,\cdot$ over the surface. The gradient $\nabla_y\,\cdot$ is then approximated at the boundary between two volumes by a finite difference. Assume that the discretization is such that two neighboring finite volumes share the membrane, i.e. one half of the thickness is in e.g. the left volume and the other half in the right volume. The flux between these two volumes is then determined by the effective diffusion coefficient D_α^{eff} for the straight path $\mathcal{C}$ between the two volume centers. The effective diffusion coefficient is given by

$$1/D_\alpha^{eff} = \int_{\mathcal{C}} D_\alpha(s)^{-1}\mathrm{d}s = \frac{h_l}{D_\alpha^l} + \frac{h_m}{D_\alpha^m} + \frac{h_r}{D_\alpha^r},$$

where the path was split into three subpaths: one left of the membrane, on the membrane and to the right of the membrane (indexed by l, m and r). Within these subpaths D_α is assumed to be constant. The paths have the lengths h_l, h_m and h_r, respectively. h_m corresponds to the membrane thickness. Using the characteristic values of the problem (cmp. Table 1), we find that $\frac{h_m}{D_\alpha^m} \gg \frac{h_l}{D_\alpha^l}$ and $\frac{h_m}{D_\alpha^m} \gg \frac{h_r}{D_\alpha^r}$, and hence with high accuracy $D_\alpha^{eff} \approx D_\alpha^m$. Hence, the thin and impermeable membranes can be treated numerically as surfaces of low permeability between two finite volume cells. The flux between two cells separated by a membrane is then proportional to the membrane diffusivity.

After solving the cell problems, the effective transport coefficients have to be determined. This was achieved by means of Eq. (12) and numerical integration. The numerical solution $(w_u)_1$ of the diffusion cell problem in y_1-direction and the solution Z_{uu} of the transport cell problem are presented in Fig. 3. The mean reaction rates are

$$\varepsilon^{-1}\langle R_d\rangle = 5 \times 10^9\ \mathrm{h}^{-1} \quad \text{and} \quad \varepsilon^{-1}\langle R_r\rangle = 4.09 \times 10^8\ \mathrm{h}^{-1},$$

which results in an equilibrium constant $\langle R_d\rangle/\langle R_r\rangle = 12.2$. Therefore in the homogenized tissue almost all auxin is dissociated. The effective diffusion coefficients are

$$\frac{\mathcal{A}_u}{D_w} = \begin{pmatrix} 0.137 & \mathcal{O}(10^{-13}) \\ \mathcal{O}(10^{-13}) & 0.67 \end{pmatrix} \times 10^{-2} \quad \text{and} \quad \frac{\mathcal{A}_v}{D_w} = \begin{pmatrix} 0.285 & \mathcal{O}(10^{-12}) \\ \mathcal{O}(10^{-12}) & 2.16 \end{pmatrix} \times 10^{-2}.$$

These are very small compared to the diffusion coefficient in water D_w. As expected diffusion is of small importance at the macroscopic scale. Due to the chosen geometry, $\mathcal{A}_{u,v}$ are diagonal up to numerical approximation errors. Diffusion in the y_2-direction is larger, because the cells are longer in this direction and thus the appearance frequency of the membranes is lower.

As far as the authors know, there are no measured values of the effective diffusivity. The reason for this becomes clear, when the accuracy of the original measurements is considered, [13]. The spatial resolution of the measurements was low, 2 mm sections were measured to obtain a profile for a 20 mm plant section. Moreover, the sensitive spatial angle of the detector might have been large, and might have resulted in also measuring the radioactivity of neighboring sections. The experimental method is good enough to determine the transport velocity of profiles, however, when it comes to obtain true dispersion coefficients, it is too imprecise. From the measurements presented in [13], one would expect to have a substantially larger diffusion/dispersion coefficient than the ones determined here. The reason for the discrepancy might be due to the low resolution of the experimental method, but probably mostly due to the high intrinsic variation found in

Please cite this article in press as: A. Chavarría-Krauser, M. Ptashnyk, Homogenization of long-range auxin transport in plant tissues, Nonlinear Analysis: Real World Applications (2009), doi:10.1016/j.nonrwa.2008.12.003

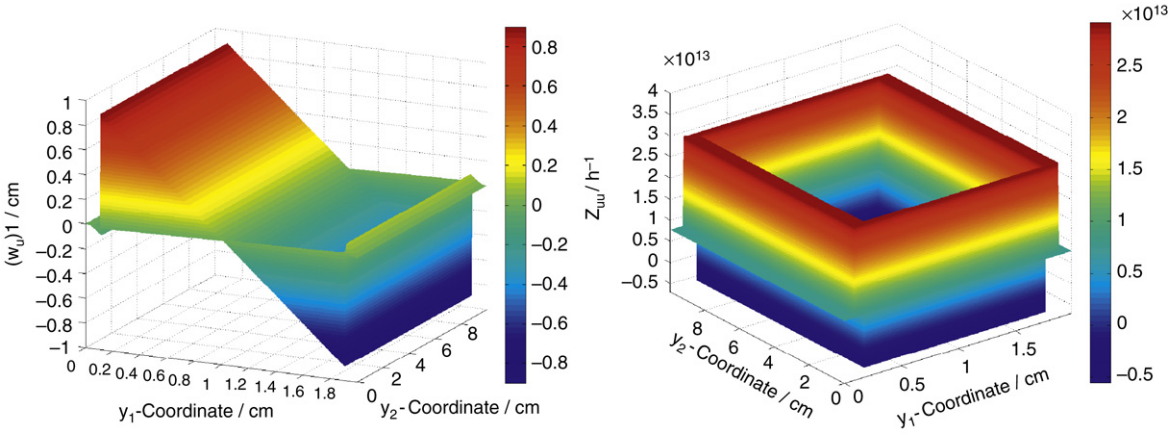

Fig. 3. Numerical simulation of the solution of the cell problems: $(w_u)_1$ (diffusion) and Z_{uu} (transport).

biological systems. Not only variations in cell form and size (up to 100% is common), but also in distribution and density of transporters are typical. Plant cells might also "sequestrate" marked auxin into their vacuoles or other organelles (a process not accounted for in the model presented here). All these processes broaden substantially an auxin peak during its transportation in the tissue, and are denominated collectively as dispersion by experimentalists. Already in [13] this theme was discussed and a contribution was attributed to diffusion (without quantification). The results found here show actually that the dispersion found in measurements cannot be explained by diffusivity and disagrees with the hypothesis posed in [13].

More important than the diffusion coefficients are the effective transport velocities, because the literature offers better results. As a consequence of the constant dissociation rate R_d and the symmetry of the selected geometry (Fig. 2), only the transport velocity $\mathcal{V}_{uu}$ is expected to be different from zero. The distribution of the permeability of the transport proteins was chosen so that transport is in y_2-direction. Both are confirmed by the numerical results

$$\mathcal{V}_{uu} = \begin{pmatrix} \mathcal{O}(10^{-4}) \\ 0.638 \end{pmatrix} \text{cm h}^{-1} \quad , \quad \mathcal{V}_{uv} = \begin{pmatrix} \mathcal{O}(10^{-11}) \\ \mathcal{O}(10^{-7}) \end{pmatrix} \text{cm h}^{-1},$$

$$\mathcal{V}_{vu} = \begin{pmatrix} \mathcal{O}(10^{-11}) \\ \mathcal{O}(10^{-7}) \end{pmatrix} \text{cm h}^{-1} \quad , \quad \mathcal{V}_{vv} = \begin{pmatrix} \mathcal{O}(10^{-8}) \\ \mathcal{O}(10^{-4}) \end{pmatrix} \text{cm h}^{-1}.$$

Measurements of pulses of radioactively labeled auxin confirm the transport velocity (measurements: 1.2–1.5 cm h^{-1}, [13]). Also the results of discrete models for root tips is within this range, [4].

Homogenization was used successfully to show that auxin transport has a transport velocity. Although the electrical field is localized to the membranes, macroscopic transport is a consequence of it. Through numerical simulation of the cell problems, the velocity was shown to be of the order of measured values. It was a priori not clear if the measured permeabilities found in the literature truly reflect the real situation, as these have been partially measured using wrong assumptions on the type of transport model.

References

[1] J. Gutknecht, A. Walter, Transport of auxin (Indoleacetic acid) through lipid bilayer membranes, J. Membr. Biol. 56 (1980) 65–72.
[2] E.M. Kramer, N.L. Frazer, T.I. Baskin, Measurement of diffusion within the cell wall in living roots of Arabidopsis thaliana, J. Exp. Bot. 58 (2007) 3005–3015.
[3] H.W. Nürnberg, G.C. Barker, The determination of the rate constants for the dissociation and recombination of weak acids by high level faradaic rectification, Die Naturwissenschaften 51 (1964) 191–192.
[4] R. Swarup, E.M. Kramer, P. Perry, K. Knox, H.M.O. Leyser, J. Haseloff, G.T.S. Beemster, R. Bhalerao, M.J. Bennett, Root gravitropism requires lateral root cap and epidermal cells for transport and response to a mobile auxin signal, Nature Cell Biol. 7 (2005) 1057–1065.
[5] W.D. Teale, I.A. Paponov, K. Palme, Auxin in action: Signalling, transport and the control of plant growth and development, Nature Rev. 7 (2006) 847–859.
[6] G.K. Muday, A. Delong, Polar auxin transport: Controlling where and how much, Trends Plant Sci. 6 (2001) 535–542.
[7] M.H.M. Goldsmith, The polar transport of auxin, Ann. Rev. Plant Physiol. 28 (1977) 439–478.
[8] M.H.M. Goldsmith, T.H. Goldsmith, M.H. Martin, Mathematical analysis of the chemosmotic polar diffusion of auxin through plant tissues, Proc. Natl. Acad. Sci. USA 78 (1981) 976–980.
[9] M.H. Martin, M.H.M. Goldsmith, T.H. Goldsmith, On polar auxin transport in plant cells, J. Math. Biol. 28 (1990) 197–223.
[10] M.H.M. Goldsmith, T.H. Goldsmith, Quantitative predictions for the chemiosmotic uptake of auxin, Planta 153 (1981) 25–33.
[11] K. Palme, L. Gälweiler, PIN-pointing the molecular basis of auxin transport, Curr. Opin. Plant Biol. 2 (1999) 375–381.
[12] G. Parry, A. Marchant, S. May, R. Swarup, K. Swarup, N. James, N. Graham, T. Allen, T. Martucci, A. Yemm, R. Napier, K. Manning, G. King, M. Bennett, Quick on the uptake: Characterization of a family of plant auxin influx carriers, J. Plant Growth Regul. 20 (2001) 217–225.
[13] M.H.M. Goldsmith, Movement of pulses of labeled auxin in corn coleoptiles, Plant Physiol. 42 (1967) 258–263.

Please cite this article in press as: A. Chavarría-Krauser, M. Ptashnyk, Homogenization of long-range auxin transport in plant tissues, Nonlinear Analysis: Real World Applications (2009), doi:10.1016/j.nonrwa.2008.12.003

[14] A. Bourgeat, M. Jurak, A.L. Piatnitski, Averaging a transport equation with small diffusion and oscillating velocity, Math. Methods Appl. Sci. 26 (2003) 95–117.
[15] A. Mikelić, V. Devigne, C.J. van Duijn, Rigorous upscaling of the reactive flow through a pore, under dominant Peclet and Damkohler numbers, SIAM J. Math. Anal. 38 (4) (2006) 1262–1287.
[16] J. Rubinstein, R. Mauri, Dispersion and convection in porous media, SIAM J. Appl. Math. 46 (1986) 1018–1023.
[17] D. Gilbarg, N.S. Trudinger, Elliptic Partial Differential Equations of Second Order, Springer-Verlag, Berlin Heidelberg, 2001.
[18] O.A. Ladyzenskaja, V.A. Solonnikov, N.N. Uralceva, Linear and Quasi-linear Equations of Parabolic Type, American Mathematical Society, 1968.
[19] G.M. Lieberman, Second Order Parabolic Differential Equations, World Scientific, Singapore, 1996.
[20] M.H.M. Goldsmith, P.M. Ray, Intracellular localization of the active process in polar transport of auxin, Planta 111 (1973) 297–314.
[21] P.S. Nobel, Physicochemical and Environmental Plant Physiology, Elsevier Academic Press, 2005.

Please cite this article in press as: A. Chavarría-Krauser, M. Ptashnyk, Homogenization of long-range auxin transport in plant tissues, Nonlinear Analysis: Real World Applications (2009), doi:10.1016/j.nonrwa.2008.12.003